UTILIZATION OF PROTON PUMP INHIBITORS IN COMBINATION REGIMEN FOR BREAST CANCER TREATMENT BY TARGETING FATTY ACID SYNTHASE

Chao Wang

Submitted to the faculty of the University Graduate School
in partial fulfillment of the requirements
for the degree
Master of Science
in the Department of Pharmacology and Toxicology,
Indiana University

November 2018

Accepted by the Graduate Faculty of Indiana University, in partial fulfillment of the requirements for the degree of Master of Science.

Master's Thesis Committee

_____
Jian-Ting Zhang, PhD, Chair

_____
Karen E. Pollok, PhD

_____
Jingyuan Liu, PhD

_____
Ahmad Safa, PhD

Dedication

I dedicate this dissertation to my wife Xi Wu, to my mother Fengying Dong, to my late father Zongyang Wang, to my daughter Ada Wang, and to my son Alexander Wang.

Acknowledgments

First and foremost, I would like to express my deepest gratitude for my mentor, Dr. Jian-Ting Zhang, for his patient and inspiring mentorship throughout my graduate life as a master student. At time of working in his laboratory, I learned a lot from him, not only the specific skills and knowledges, but also the scientific mind, the ability of solving problems, and the dedication to medical science. His trust, help and guidance meant so much to me when I had difficulties.

I would like to also thank my committee member, Dr. Jingyuan Liu. During the time working with her, I gained precious experiences in protein purification. I would also like to acknowledge my committee administrative chair Dr. Ahmad Safa and committee member Dr. Karen Pollok for serving on my thesis committee and providing me great suggestions and advice.

I would like to express my special gratefulness to Dr. Zizheng Dong for teaching me lab skills and sharing with me his valuable experiences. I would like to give my sincere thanks to the many members past and present of Dr. Zhang's lab and Dr. Liu's lab. Thanks to Valerie Fako for her previous PPI work, which made this study possible. Thanks to Yifan Chen who taught me to culture my first-ever flask of breast cancer cells. Thanks to Wendy Zhang for helping me with the flow cytometry and confocal microscopy work. Thanks to Deren Li for collaborating patient data analysis for this study. Special thanks go to my late friend, Jing Qi, who gave me tremendous amount of help both in and out the lab.

Lastly, I would like to express my deepest gratitude to my family members for all their support and encouragement, especially to my wife Xi Wu, who is always there for me,

understands me, supports me, helps me, believes in me, and gave birth to our wonderful children, Ada and Alexander.

It has been a great journey which means way more than a degree to me. And I will always remember all the kindness and help I received from people who shared this trip with me. Thank you all!

Chao Wang

UTILIZATION OF PROTON PUMP INHIBITORS IN COMBINATION REGIMEN FOR BREAST CANCER TREATMENT BY TARGETING FATTY ACID SYNTHASE

Fatty acid synthase (FASN) over-expression has been associated with poor prognosis and recurrence in cancer patients. In addition, it has also been found that overexpression of FASN causes resistance to DNA-damaging treatments by up-regulating the non-homologous end joining (NHEJ) repair of DNA double-strand break.

Proton pump inhibitors (PPIs), were originally designed to decrease gastric acid production by binding irreversibly with gastric hydrogen potassium ATPase. PPIs have recently been reported to reduce drug resistance in cancer cells when used in combination with other chemotherapeutics, although the mechanism of resistance reduction is uncertain. In our lab, previous investigation showed that PPIs decreased FASN thioesterase (TE) domain activity and cancer cell proliferation in a dose-dependent manner.

In this study, I tested the hypothesis that PPIs sensitize breast cancer cells to doxorubicin and ionizing radiation (IR) treatments by inhibiting FASN. When administered to breast cancer cells as single-agent, lansoprazole exhibited the highest potency in inhibiting both FASN activity and breast cancer cell proliferation, among four PPIs tested. In addition, treatment of breast cancer cells with lansoprazole decreased the mRNA and protein levels of poly (ADP-ribose) polymerase-1 (PARP-1) and NHEJ activity, accompanied by elevated γ-H2AX expression. Following a 3-day treatment with lansoprazole, a dose-dependent disruption in cell cycle disruption and increased apoptosis were also detected. Combination

of lansoprazole with either doxorubicin or IR caused profoundly higher levels of DNA damage accumulation than doxorubicin or IR treatment alone, suggesting synergistic effects.

Taken together, our observations suggest that PPIs synergistically suppress breast cancer cells in combination with DNA damaging treatments by inhibiting FASN. These findings may provide a potential route to overcome resistance to DNA-damaging chemo/radiation treatments in refractory breast cancers.

Jian-Ting Zhang, PhD, Chair

Table of Contents

List of Tables

List of Figures

List of Abbreviations

BER:	Base excision repair
BSA:	Bovine serum albumin
CI:	Combination index
DAPI:	4',6-diamidino-2-phenylindole
DDR:	DNA damage respond
DMSO:	Dimethyl sulfoxide
Dox:	Doxorubicin
DSB:	DNA double strand break
DTT:	Dithiothreitol
EDTA:	Ethylenediaminetetraacetic acid
FA:	Fatty acid
FASN:	Fatty acid synthase
FDA:	Food and drug administration
HR:	Homologous recombination
IR:	Ionizing radiation
Lan:	Lansoprazole
NADPH:	Nicotinamide adenine dinucleotide phosphate
NHEJ:	Non-homologous end joining
NS:	Not significant
Ome:	Omeprazole
OTC:	Over the counter
Pan:	Pantoprazole

PARP:	Poly (ADP-ribose) polymerase
PBS:	Phosphate buffered saline
rt-qPCR:	Real-time quantitative polymerase chain reaction
PI:	Propidium iodide
PMSF:	Phenylmethylsulfonyl fluoride
PPI:	Proton pump inhibitor
PVDF:	Polyvinylidene difluoride
Rab:	Rabeprazole
SDS:	Sodium dodecyl sulfate
SD:	Standard deviation
TBS:	Tris buffered saline
TBST:	Tris buffered saline with Tween-20
TE:	Thioesterase

Introduction

A. Brief overview of fatty acid synthase

Fatty acid synthase (FASN), a 270-kDa homodimeric enzyme, is the sole mammalian enzyme involved in *de novo* lipid biosynthesis. It is a seven-domain enzyme that catalyzes the synthesis of saturated long-chain fatty acids, mainly 16-carbon palmitate, from acetyl CoA and malonyl CoA, utilizing nicotinamide adenine dinucleotide phosphate (NADPH) as reducing agent [1-4]. Lipids play important roles in energy metabolism and storage, also as signaling molecules, including sterols, isoprenoids, acylglycerols and phospholipids [5-8]. *De novo* fatty acid biosynthesis is largely repressed by dietary fat in normal tissues, restricted mainly to lipogenic tissue, liver, and lactating breast. In contrast, cancer cells are often found to have elevated FASN expression and activity, which could be a response to the high metabolic demand and low availability of serum-derived lipids in the tumor microenvironment [5-13]. Numerous studies have shown that highly activated FASN was found in many cancer types compared with normal tissues, notably in breast cancers [14-19]. Fatty acid synthesis is crucial for cancer cell development, growth, maintenance and survival. Moreover, FASN over-expression has also been associated with poor prognosis and recurrence in cancer patients [20, 21].

In our lab, it has been found that overexpression of FASN contributes to resistance to DNA-damaging treatments, such as doxorubicin, mitoxantrone, etoposide, and ionizing radiation (IR). Later studies showed that FASN regulated cellular response against genotoxic insults by up-regulating poly (ADP-ribose) polymerase-1 (PARP-1) and DNA repair. Overexpression of FASN suppressed NF-κB but increased SP1 expression. SP1 competes with NF-κB in binding to the composite element of the PARP-1 promoter and

led to up-regulation of PARP-1. PARP-1 increased Ku protein recruitment and DNA repair activity. Lipid deprivation had no effect on NF-κB but suppressed SP1 expression, which could be rescued by palmitate supplementation [22-24].

B. Brief overview of PARP and DNA repair

Poly (ADP-ribose) polymerases (PARPs) are ADP-ribosyl transferase enzymes that transfer negatively charged ADP-ribose groups to itself and other target proteins from donor NAD+, a process called PARylation. Through PARylation, PARPs play crucial roles in a variety of cellular processes, such as transcriptional regulation, RNA interference, mitochondrial function, formation of subnuclear bodies and cell division, most prominently in DNA damage response (DDR). In humans, PARP-1, the most characterized member of the PARP superfamily accounts for more than 90% of overall cellular PARylation activity in response to DNA damage. At sites of DNA breaks, autoPARylation of PARP serves as a signal and recruits DNA repair machinery to the damage site to activate DNA repair processes. Accumulation of negative charges from autoPARylation drives PARP to dissociate from DNA, which is required for DNA repair completion [25-27].

PARP has been demonstrated to be involved in most DNA repair pathways, including base excision repair (BER), homologous recombination (HR), and non-homologous end joining (NHEJ) processes. NHEJ, despite its error-prone nature and elevated inaccuracy, is the predominant repair pathway for double-strand breaks (DSBs) in mammalian cells for its rapid repair activity and being active throughout the cell cycle [28]. There are accumulating reports showing that PARP-1 acts as sensors of DSBs in the genome by

binding to the break and recruiting different downstream repair proteins of both the HR and NHEJ pathways [24, 29].

C. Brief overview of FASN inhibitors and proton pump inhibitors

FASN was first identified as tumor antigen OA519 in aggressive breast cancers in 1994 [30]. Over the past twenty years, the importance of fatty acid biosynthesis for cancer cell growth and survival has been shown in numerous studies, and many different inhibitors of FASN have been developed and evaluated, such as cerulenin [30-32], C75 [33-38], orlistat [39-41], and triclosan [42-44]. Despite the promising potential of FASN as a target against cancers, there is only one FASN inhibitor, TVB-2640, that entered clinical trial [45]. The difficulty in selectively inhibiting fatty acid biosynthesis in cancer cells without dramatic systemic effects was a major issue that needs to be conquered. To search for novel inhibitors of FASN while minimizing unwanted side effects, our lab tried to reposition FDA-approved drugs, which are well-studied in patients, as FASN inhibitors. Virtual DOCK screening of FDA-approved drugs followed by a fluorogenic assay using recombinant thioesterase (TE) protein led to the finding that proton pump inhibitors (PPIs) competitively inhibited FASN TE activity [46].

PPIs, among the most widely sold drugs in the world, effectively reduce stomach acid production. They are OTC drugs and generally well tolerated in human. PPIs are prodrugs which are activated by acid, and bind covalently to the gastric H+, K+-ATPase via disulfide bond [47]. Recently, PPIs have been reported to sensitize cancer cells when used in combination with other chemotherapeutics, although the mechanism of action is uncertain [48-53].

Previous study in our lab showed that PPIs were able to decrease FASN activity and cancer cell proliferation [46]. In this study, the objective was to expand our studies focused on the effectiveness of PPIs in targeting FASN in breast cancer cells. In addition, how PPIs mechanistically impact PARP-1 level and DNA repair activity through FASN inhibition was further investigated. Finally, the most potent PPI identified in this study was evaluated in combination with standard-of-care DNA-damaging agents used to treat breast cancer to evaluate potential synergistic effects in suppressing breast cancer growth.

Materials and Methods

A. Materials

Cell culture mediums Opti-MEM and fetal bovine serum were purchased from Life technologies (Grand Island, NY). DMEM, trypsin-versene mixture, and Antibiotic/Antimycotic solution 100x were purchased from Mediatech (Manassas, VA), Lonza (Walkersville, MD) or GE (Logan, UT). pGL3 Luciferase Reporter Vectors, pRL *Renilla* Luciferase Control Reporter Vectors, and Dual-Luciferase Reporter Assay System were purchased from Promega (Madison, WI). All electrophoresis reagents, polyvinylidene difluoride (PVDF) membranes were purchased from Bio-Rad (Hercules, CA). Lansoprazole, omeprazole, pantoprazole, rabeprazole, doxorubicin, PMSF, dithiothreitol (DTT), and propidium iodide (PI) were purchased from Sigma (St. Louis, MO). Annexin V-FITC apoptosis detection kit was purchased from Millipore (Billerica, MA). Olaparib was purchased from LC Laboratories (Woburn, MA). SYBR Green PCR master Mix for rt-qPCR was purchased from Applied Biosystems (Foster City, CA). Monoclonal antibody against fatty acid synthase (FASN) was purchased from BD Biosciences (San Jose, CA). Antibodies to PARP-1, was purchased from Cell Signaling (Danvers, MA). γ-H2AX antibody was purchased from Millipore (Billerica, MA). Lipofectamine 2000 and G418 were purchased from Life technologies (Grand Island, NY). ECL Western Blotting detection reagents and SuperSignal West Dura extended duration substrate were purchased from GE Healthcare (Pittsburg, PA) and Thermo Scientific (Rockford, IL), respectively. MCF7, MDA-MB-468, and MDA-MB-231 cells were purchased from ATCC (Manassas, VA). T47D cells were generously provided by Dr. Brittney-Shea Herbert (IUSM).

B. Cell culture

Human breast cancer cell line MCF7, T47D, MDA-MB-468, and MDA-MB-231 were cultured at 37 °C with 5% CO_2 in DMEM medium, supplemented with 10% fetal bovine serum and 1x Antibiotic/Antimycotic solution. FASN-overexpressing MCF7 clones (MCF7/FASN) and its vector-transfected control clones (MCF7/Vec) were maintained in DMEM medium supplemented with 10% fetal bovine serum, 1x Antibiotic/Antimycotic solution, and 400 μg/ml G418. Doxorubicin resistance stable clones MCF7/AdVp3000 with FASN-knockdown (M3k/SiFASN) and its control scrambled shRNA-transfected clone (M3k/Scr) were maintained in DMEM medium supplemented with 10% fetal bovine serum, 1x Antibiotic/Antimycotic solution, 400 μg/ml G418, and 3000 ng/L doxorubicin. G418 and doxorubicin were not included in the experimental treatment media.

C. Western blot analysis

Cells were harvested and then lysed in TNN buffer (50 mM Tris-HCl, 150 mM NaCl, 0.5 % NP-40, 5 mM EDTA, 50 mM NaF, 1 mM Na3VO3, with 1 mM PMSF and 1 mM DTT, added immediately before use, pH = 7.4) for 30 min on ice with occasional agitation. After brief sonication, lysate was harvested and centrifuged at 13,000 g for 15 minutes at 4 ºC to remove insoluble pellet. Protein concentration of cell lysate was determined using Bio-Rad protein assay kit. Cell lysates were resolved by SDS-PAGE followed by transferring to a polyvinylidene fluoride membrane. The blot was then probed with antibodies as follows: Fatty Acid Synthase (610963, BD biosciences), PARP-1 (46D11, CST), β-actin (A2228, Sigma), γ-H2AX (05-636, Millipore) and horseradish peroxidase–conjugated secondary antibodies (Sigma). The signal was captured by X-ray films after

incubation with Amersham ECL Western Blotting Detection Reagent (RPN2106, GE). X-ray films were scanned and quantified with ImageJ.

D. FASN activity assay

FASN holoenzyme activity was measured by NADPH oxidation of fatty acid synthesis as previously described [54]. From a group of four breast cancer cell lines, MCF7 lysate was chosen to test FASN activity for its high FASN expression level. MCF7 cells were detached by digestion with Trypsin + EDTA (0.05%), washed with PBS and resuspend in ice-cold PBS buffer containing 1 mM DTT, 1 mM EDTA, and 0.05% Brij35. After brief sonication, lysate was harvested and centrifuged at 13,000 g for 15 minutes at 4 ºC to remove insoluble pellet. Protein concentration of cell lysate was determined using Bio-Rad protein assay kit. In each well of a 96-well flat bottom plate, 250 µg total protein was used in 200 µL reaction consisting of 200 mM K_2HPO_4 pH6.8, 1 mM DTT, 1 mM $MgCl_2$, 240 µM NADPH, and 30 µM Acetyl-CoA. After incubation with various concentrations of compounds or DMSO for 10 min at 37 °C, malonyl-CoA was added to a final concentration of 50 µM to start the reaction. Absorbance at 340 nm was measured every minute for 20 min. Results were analyzed and IC_{50}s were calculated by Prism 7.0 (GraphPad, La Jolla, USA). Experiments were performed in duplicate of three independent experiments.

E. Colony formation assay

Breast cancer cells were seeded in six-well plates at density of 200 cells/well and cultured overnight. Cells were given serial concentrations of compounds or DMSO (final concentration 0.5%) and cultured for 14 days. Generated colonies were washed by PBS,

fixed in 100% methanol and stained with 0.5% crystal violet in 25% methanol. Excess dye was removed by wash the plates with water. Colonies were manually counted. Concentration-response curves and respective IC_{50} values were calculated using Prism 7.0. Experiments were performed in triplicate wells for each condition and repeated at least three times.

F. Methylene blue assay

Breast cancer cells were seeded in 96 well plates at density of 2000 cells/well and cultured overnight. Serial concentrations of compounds or DMSO were given to treat the cells and cells were cultured for 3 days. Media was then removed, and cells were washed with saline and fixed in 100% methanol. Each well was stained with 1% w/v methylene blue in 10 mM borate buffer (pH 8.5) and allow incubation for 30 min. After removing excess dye and washing the cells with 10 mM borate buffer (pH8.5), 100 μL 1:1 (v/v) 100% ethanol: 100 mM HCl mixture was added to each well to release dye. Plates were gently shaken and read the absorbance at 650 nm. Concentration-response curves and respective IC_{50} values were calculated using Prism 7.0. Experiments were performed in triplicate wells for each condition and repeated at least three times.

G. Real-time quantitative PCR analysis

rt-qPCR was performed as described previously [23, 24]. Briefly, treated cells were harvested, and total RNA was extracted using PureLink RNA Mini Kit (Life technologies, Grand Island, NY). Total cellular RNA then was reverse transcribed into complementary DNA (cDNA) by using iScrpt cDNA synthesis kit (Bio-Rad, Hercules, CA). Rt-qPCR was

performed using SYBR Green PCR Master Mix (Applied Biosystems, Carlsbad, CA) on StepOnePlus real time PCR system. Experiments were performed in triplicate.

H. Immunofluorescence imaging

Breast cancer cells were seeded in Nunc Lab-Tek II Chamber Slide (Thermo Scientific, Rockford, IL) at density of 50,000 cells/well and treated with 10 μM lansoprazole or DMSO twice a day for 3 days. Cells were washed with PBS and fixed with 50%:50% (v/v) Acetone/Methonal at room temperature for 10 minutes. Cells were permeabilized using 1 ml Triton X-100/PBS (0.5% v/v). Non-specific protein binding was blocked with 1 ml of BSA (1% v/v). Primary γ-H2AX antibody (diluted 1:500 in 1% BSA; Millipore) was added to each well for one-hour incubation at room temperature. Followed by secondary Anti-mouse-IgG-FITC antibody (diluted 1:500 in 1% BSA, Sigma) for 45 minutes at room temperature in the dark and washed twice with PBS. The cells were counter stained with DAPI and stored in the dark at 4 °C before viewing on a confocal microscope [24].

I. Host cell reactivation NHEJ assay

The host cell reactivation NHEJ assay was carried out as previously described[24] with minor modifications. Briefly, 1×10^4 cells were seeded in 24-well plates, cultured overnight and then treated with 10 μM lansoprazole or DMSO twice a day for 3 days before transfected with 400 ng linearized or intact pGL3-luc firefly luciferase plasmids using Lipofectamine 2000 (Invitrogen). pGL3-luc plasmid was linearized by HindIII digestion, and linearization was verified by DNA agarose gel electrophoresis before transfection. 400 ng pRL-TK (Promega) plasmid which encodes renilla luciferase was co-transfected as a

control for transfection efficiency. 8 hours after transfection, cells were harvested and assayed for luciferase activity with Dual Luciferase Assay (Promega) on a luminometer. Firefly luciferase signal were normalized to renilla luciferase signal in each group. Overall NHEJ activity was calculated by firefly luciferase activity from cells transfected with linearized plasmid relative to cells transfected with intact plasmid. Experiments were performed in triplicate.

J. Flow cytometry assay

Breast cancer cells were seed in 6-well plates at 2×10^5 cells/well and followed by 3-day treatment with 10 μM lansoprazole or DMSO twice a day. To detect apoptosis, cells were collected and stained with Annexin V-FITC apoptosis detection kit (Millipore, Billerica, MA). For cell cycle analysis, cells were fixed with ice cold 70% ethanol overnight and counter stained with propidium iodide (PI) for 30 min in the dark. Apoptosis and cell cycles were analyzed by flow cytometry.

K. Combination studies

Combined effects of lansoprazole and doxorubicin were determined using colony formation assays. After concentration-response curves and respective IC_{50} values were obtained from single drug treatments, three combinations with different constant potency ratios ($IC_{50\ Lansoprazole}/IC_{50\ Doxorubicin}$) at 1:1, 1:3, and 3:1 were tested. For each potency ratio, combination index (CI) of different fractional effect was calculated for synergistic effects using isobologram and combination-index analysis. Experiments were performed in triplicate wells for each condition and repeated at least three times.

L. Isobologram and combination-index analysis

Data obtained from colony formation assay were used to determine drug synergy by isobologram analysis and combination-index analysis developed by Greco and Chou [55-58]. Isobolograms were constructed for defined growth inhibiting effects of two drugs. The line of additivity was constructed by connecting two points with the same level of growth inhibition generated as single agent. Concentrations of the two drugs used in combination to provide the same effect are shown in the same plot. Synergy, additivity, or antagonism is indicated when this point is located below, on, or above the line, respectively. The combination index values were calculated using the equation:

$$\mathrm{CI} = \frac{\mathrm{C_{A,X}}}{\mathrm{IC_{X,A}}} + \frac{\mathrm{C_{B,X}}}{\mathrm{IC_{X,B}}}$$

where $C_{A,X}$ and $C_{B,X}$ are the concentration of drug A and B used in combination to produce an effect x. $IC_{X,A}$ and $IC_{X,B}$ are the corresponding concentrations of drug A and B that produce the same effect as a single agent. CI = 1 indicates an additive effect between two drugs, whereas CI < 1 or CI> 1 indicates synergy or antagonism, respectively.

M. Ionize irradiation

1×10^6 breast cancer cells were seeded in 100 mm culture dish and treated with 10 μM lansoprazole or DMSO twice a day for 3 days. Cells were then suspended and plated in 6-well plates at density of 200 cells/well. Pre-treated group and control group received a serial dose of ionize irradiation and cultured for 14 days. Generated colonies were fixed, stained and counted manually. Concentration-response curves and respective IC_{50} values were calculated using Prism 7.0. Experiments were performed in triplicate wells for each condition and repeated at least three times.

Results

A. PPIs inhibit FASN holoenzyme activity

In a previous study, it was reported that the FDA-approved PPIs inhibited the activity of recombinant FASN TE domain in a dose-dependent manner *in vitro* [46]. It is necessary to determine whether FASN holoenzyme activity is also inhibited by PPIs in breast cancer cells. For this purpose, I performed NADPH oxidation assay using lysate from MCF7 cells, which expressed high levels of endogenous FASN. The assay is based on FASN's ability to utilize NADPH as reducing agent during lipid synthesis. Thus, incremental decrease in NADPH levels represents on-going FASN holoenzyme activity. As shown in Figure 1 and Table 1, all four PPIs inhibited FASN activity in a dose-dependent manner with IC_{50} ranging from ~6 to 18 μM. Lansoprazole and rabeprazole showed superior potency than omeprazole and pantoprazole. These observations indicate that PPIs can inhibit full length FASN enzymatic activity in breast cancer cells.

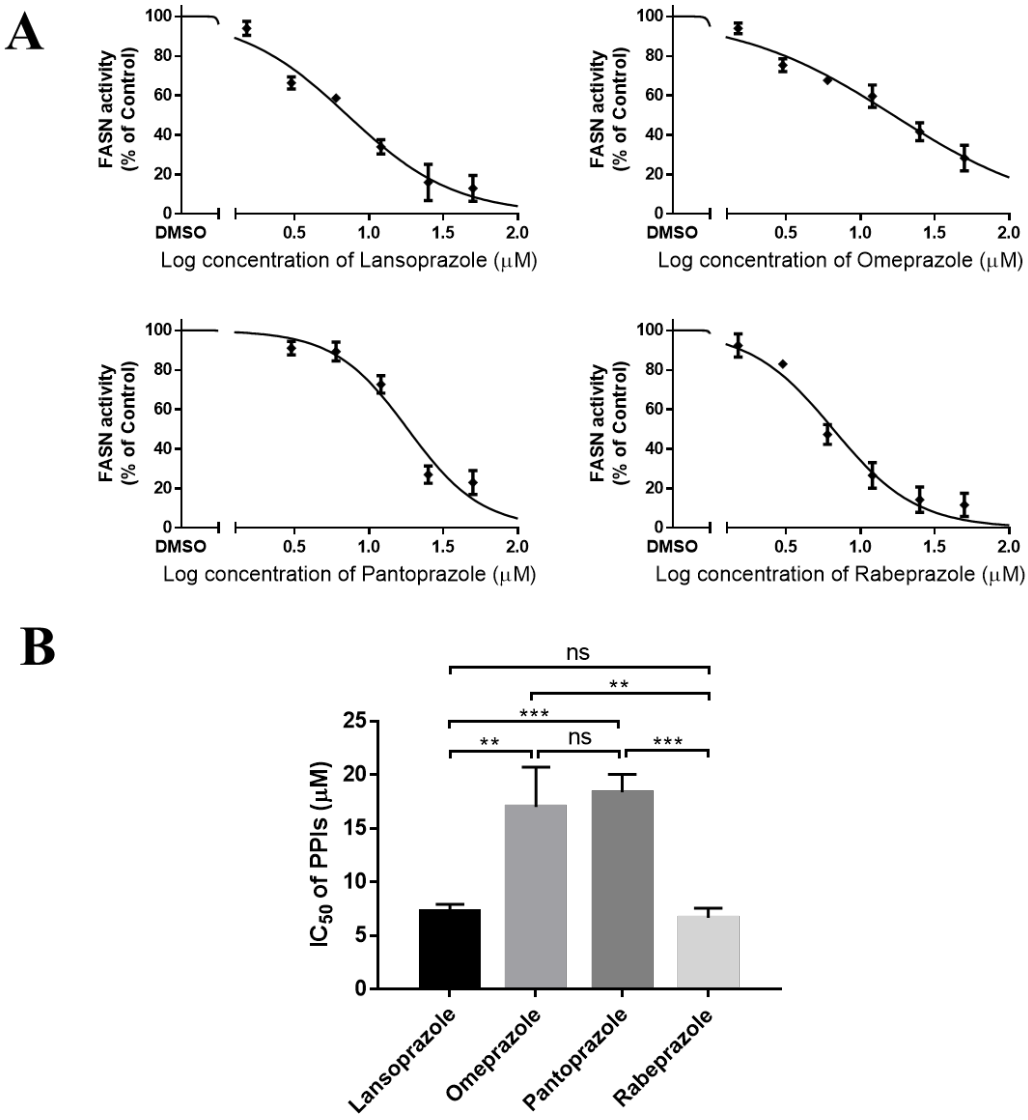

Figure 1: PPIs inhibited FASN holoenzyme activity. (A) Dose dependent curves obtained from NADPH oxidation assay for lansoprazole, omeprazole, pantoprazole, and rabeprazole. (B) IC_{50} of FASN activity inhibited by each PPI. Each data point represents the mean ± standard deviation (SD) of three independent experiments performed in duplicate. ** $P < 0.01$; *** $P < 0.001$.

TABLE 1: IC_{50} values of PPIs from NADPH oxidation assay.

PPI	Structure	IC_{50} (μM)
Lansoprazole		7.26 ± 0.65
Omeprazole		16.99 ± 3.73
Pantoprazole		18.36 ± 1.67
Rabeprazole		6.65 ± 0.91

B. PPIs inhibited breast cancer cell survival

De novo fatty acid biosynthesis has previously been shown to be necessary for survival of breast cancer cells and inhibition of FASN induces cell death. To determine if PPIs can suppress breast cancer cell survival, colony formation assays were performed using MCF7, T47D, MDA-MB-468, and MDA-MB-231 cells in the presence or absence of serially-diluted concentrations of the four PPIs. As shown in Figure 2, all four PPIs dose-dependently inhibited survival of all four breast cancer cell lines. Lansoprazole was consistently the most potent inhibitor in all four cell lines tested, with IC_{50} values of 1.28 μM in MCF7 cells, 7.61 μM in T47D cells, 3.67 μM in MDA-MB-468 cells, and 21.35 μM in MDA-MB-231 cells (Table 2).

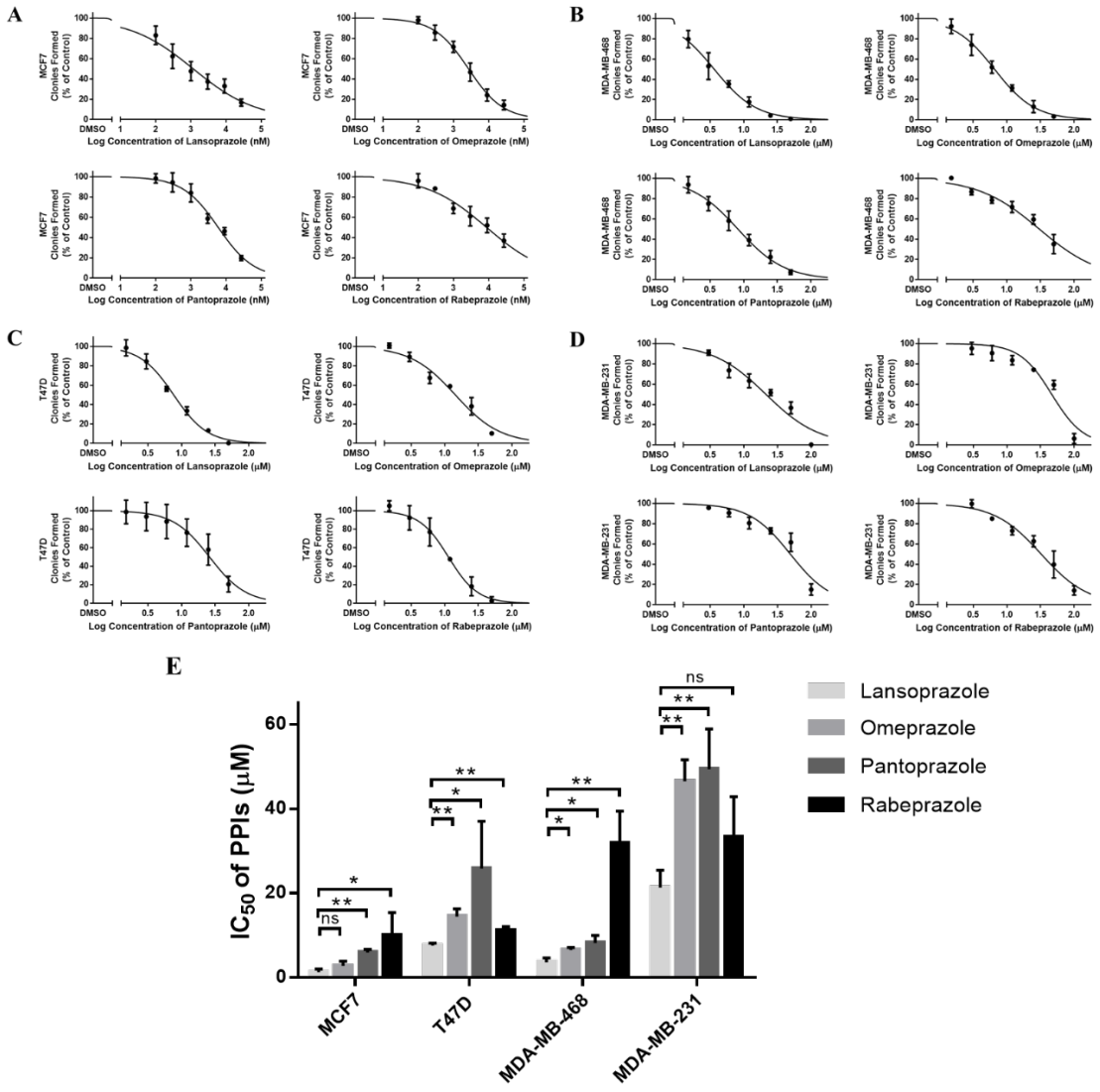

Figure 2: PPIs inhibited breast cancer cell survival. MCF7 (A), T47D (B), MDA-MB-468 (C), and MDA-MB-231 (D) cells were treated with each PPI alone and survival was measured using a colony-formation assay. Survival curves are shown and expressed as % of colonies in untreated controls. The IC_{50} of each cell line to different PPI is shown in (E). Each data point represents the mean ± SD of three independent experiments performed in triplicate. * $P < 0.05$; ** $P < 0.01$.

TABLE 2: IC_{50} values of PPIs in breast cancer cell lines obtained from colony formation assay.

	Lansoprazole (μM)	Omeprazole (μM)	Pantoprazole (μM)	Rabeprazole (μM)
MCF7	1.28 ± 0.74	2.80 ± 1.11	5.90 ± 0.73	9.96 ± 5.44
T47D	7.61 ± 0.56	14.49 ± 1.80	25.87 ± 11.15	11.16 ± 0.92
MDA-MB-468	3.67 ± 0.97	6.50 ± 0.64	8.21 ± 1.75	31.85 ± 7.63
MDA-MB-231	21.35 ± 4.09	46.48 ± 5.14	49.37 ± 9.54	33.33 ± 9.49

C. Sensitivity to PPIs correlates with endogenous relative FASN level

In the colony formation assay, I observed that cell lines with higher endogenous FASN level were more sensitive to PPI treatment, as shown by their lower IC_{50} values. The IC50s of lansoprazole, omeprazole, and pantoprazole had strong correlations with relative FASN level with coefficient of determination (R^2) of 0.99, 0.99, and 0.96, respectively (Figure 3). Rabeprazole showed less correlation with FASN expression level than the other three PPIs. Therefore, lansoprazole, which has the best potency and a strong correlation with endogenous FASN level, was chosen in the following mechanistic and combination studies.

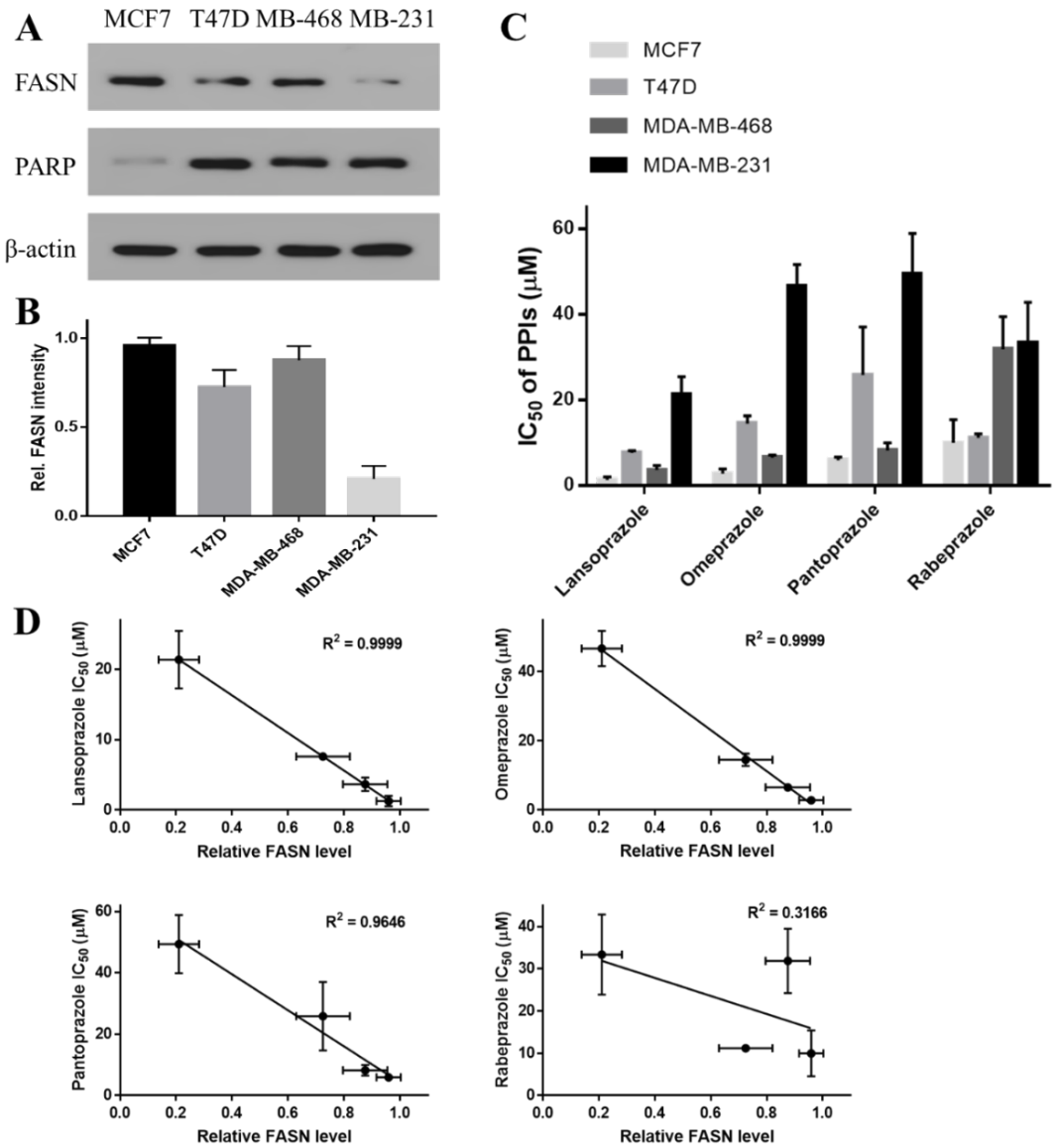

Figure 3: Correlation analysis of relative FASN level to IC_{50} of each PPI from colony formation assay. (A) Western blot analysis of FASN, PARP-1, and β-actin in MCF7, T47D, MDA-MB-468, and MDA-MB-231 cells. (B) Quantitation of relative FASN levels in four cell lines. FASN levels were quantitated using ImageJ and normalized to β-actin. The IC_{50}s of each PPI to inhibit different breast cancer cell lines are shown in (C). Correlation analyses of relative FASN levels to IC_{50}s of each PPI are shown in (D). Each point is shown as the average of three independent experiments ± SD.

D. Lansoprazole reduces mRNA and protein levels of PARP-1

Previous study in our lab has shown that over-expressing FASN up regulated PARP-1 level, which contributed to DNA-damaging treatment resistance [24]. To test whether inhibition of FASN by lansoprazole reduces PARP-1 level, MCF7 and MDA-MB-468 cells were treated with various concentrations of lansoprazole for 3 days. Cells were collected and analyzed by western blot and rt-qPCR to detect the change of PARP-1 at mRNA and protein levels after lansoprazole treatment. As shown in Figure 4, PARP-1 protein decreased dose-dependently after lansoprazole treatment (Figure 4A). PARP-1 mRNA levels were also significantly reduced after treatment with 10 μM Lansoprazole for 3 days in both cell lines (Figure 4B).

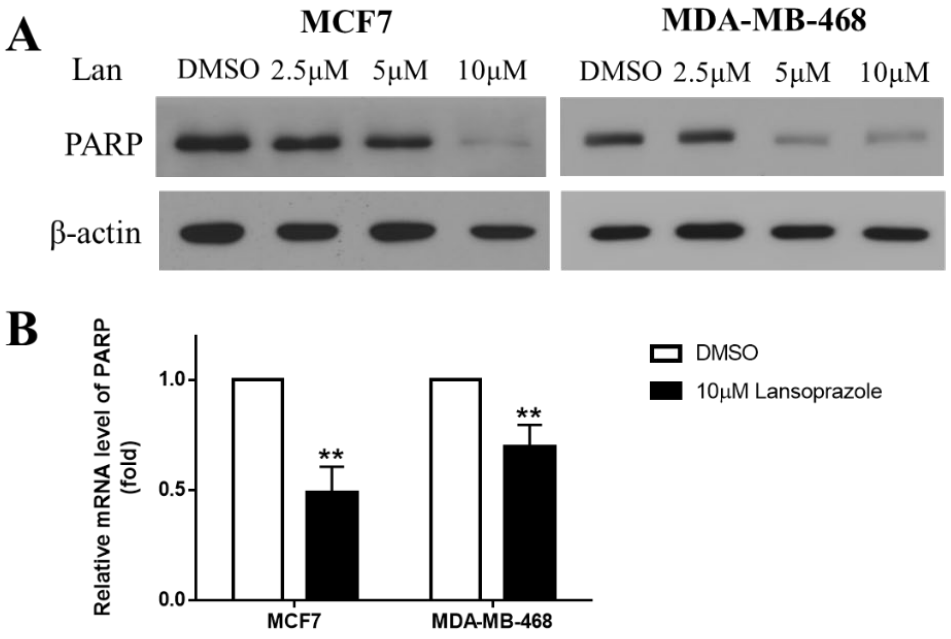

Figure 4: Effect of lansoprazole treatment on PARP-1 levels in MCF7 and MDA-MB-468 cells. (A) Western blot analysis of PARP-1 and β-actin after treating cells with different concentrations of lansoprazole or DMSO for 3 days. (B) Relative mRNA levels of PAPR-1 normalized to GAPDH from rt-qPCR after treating breast cancer cells with 10 μM lansoprazole or DMSO for 3 days. Each bar is shown as the average of three independent experiments ± SD. ** $P < 0.01$.

E. Lansoprazole reduces NHEJ repair activity

Since inhibition of FASN by lansoprazole reduces PARP-1 level, a critical protein involved in DNA repair pathways, I next tested whether lansoprazole treatment could reduce NHEJ repair activity, the predominant form of DSB repair. Utilizing a host cell reactivation-based *in vitro* NHEJ assay, I found that NHEJ activity was significantly decreased after lansoprazole treatment, by 56% and 43% in MCF7 cells and MDA-MB-468 cells, respectively (Figure 5). This observation suggests that treating breast cancer cells with lansoprazole could decrease their NHEJ DNA repair activity.

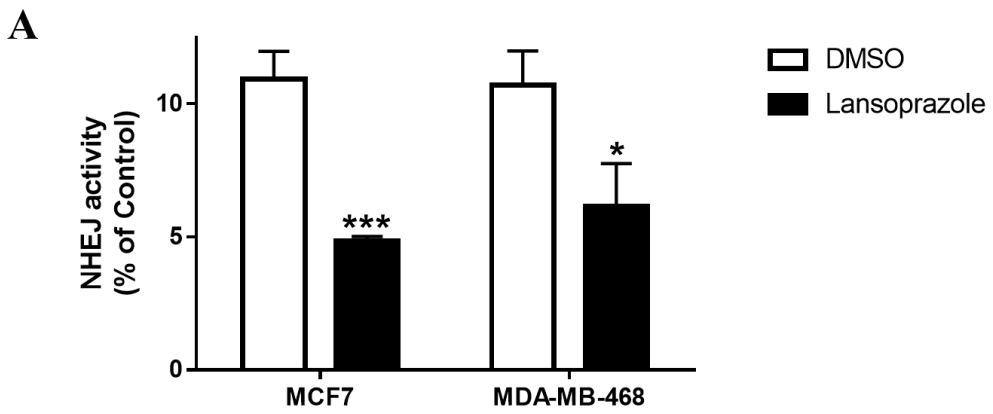

Figure 5: Effect of lansoprazole treatment on NHEJ repair activity. MCF7 and MDA-MB-468 cells were tested for their NHEJ activity using a host cell reactivation-based NHEJ assay after treating cells with 10 μM lansoprazole or DMSO for 3 days. Firefly luciferase activity was measured in both control and test groups of each cell line at 8 hours after transfection and normalized to renilla luciferase activity. NHEJ activity = (Firefly luciferase activity in test group) / (Firefly luciferase activity in control group) *100%. Each bar is shown as the average of three independent experiments ± SD. * $P < 0.05$; *** $P < 0.001$.

F. Lansoprazole promotes γ-H2AX accumulation

Due to constitutive growth signaling and defective DNA damage response, cancer cells exhibit "replication stress", which leads to DNA damage and defective replication [59]. DSB repair is critical for maintaining genome stability even without DNA damaging agents or radiation. With the compromised DSB repair activity, DNA damage can accumulate [60, 61]. Previous results suggest that FASN inhibition down-regulates PARP-1 and therefore decreases NHEJ activity [24]. I next examined whether knocking down or inhibiting FASN will affect γ-H2AX level, a marker of DNA double strand break, using western blot and immunofluorescence staining. After knocking down FASN using 100nM siRNA for 2 days, reduced PARP-1 level and increased γ-H2AX level were observed in both MCF7 and MDA-MB-468 cells, compared to the cells transfected with scrambled siRNA (Figure 6A). After treating MCF7 and MDA-MB-468 cells with 2.5 μM, 5 μM, or 10 μM lansoprazole for 3 days, γ-H2AX levels increased dose-dependently, compared to the low background levels in control cells as determined by western blot analysis (Figure 6B). In addition, I also performed immunofluorescence (IF) staining to visualize γ-H2AX levels in the nuclei of each individual cell. Increased levels of γ-H2AX foci were clearly present in lansoprazole treated cells (Figure 6C), which was consistent with the western blot results.

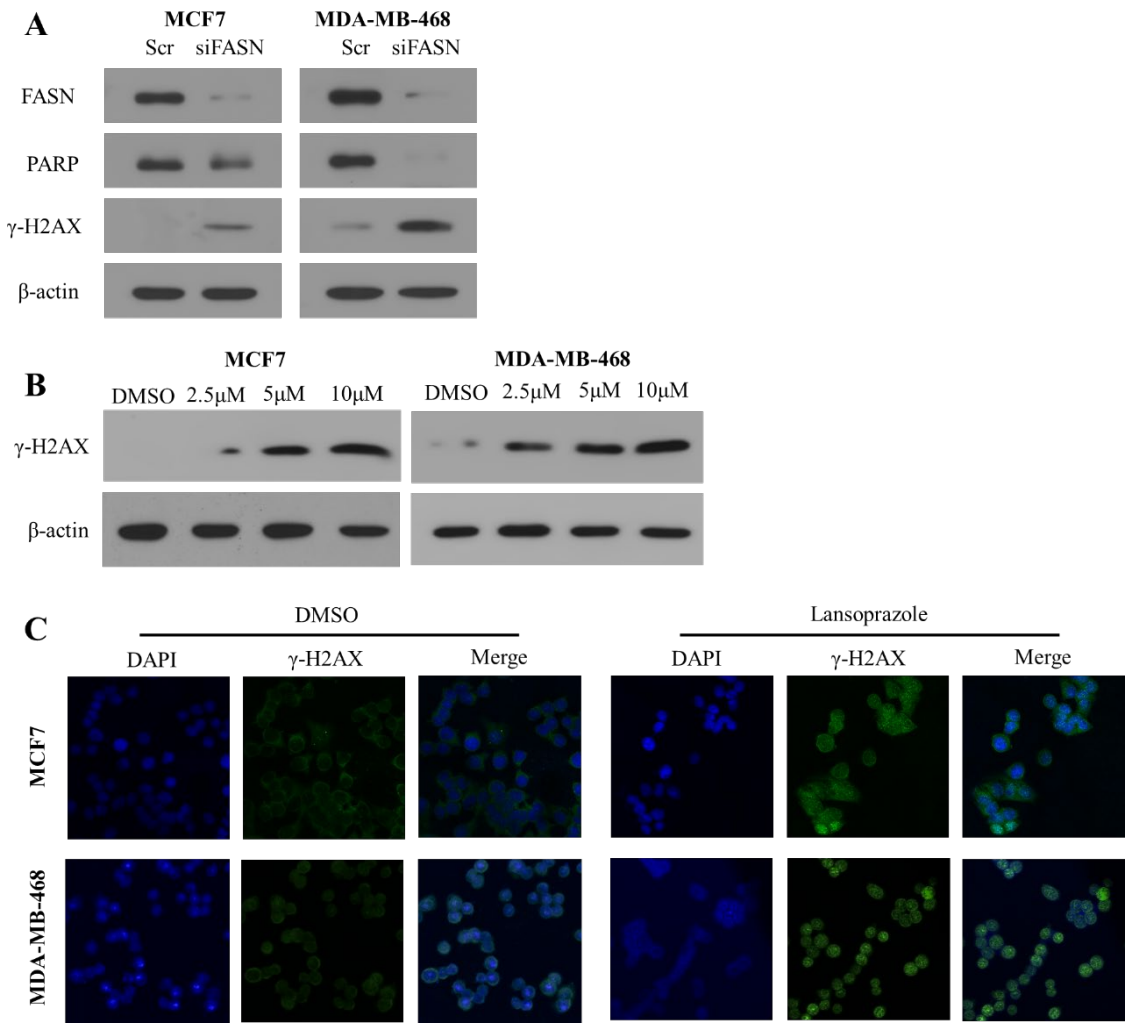

Figure 6: Effect of FASN knock-down and lansoprazole treatment on γ-H2AX level. (A) Western blot analysis of γ-H2AX after knocking down FASN using siRNA in MCF7 and MDA-MB-468 cells for 2 days. (B) Western blot and (C) immunofluorescence staining analyses of γ-H2AX in MCF7 and MDA-MB-468 cells with 3-day lansoprazole treatment.

G. FASN is a mediator of the anti-cancer effect of lansoprazole and olaparib

To determine whether FASN mediates the anti-cancer activity of PPIs, the impact of varying FASN levels to the sensitivity of lansoprazole was tested using a stable clone of MCF7 cells with FASN-overexpression (MCF7/FASN) and a stable clone of doxorubicin resistance MCF7 cells with FASN knockdown (M3K/shFASN), with their respective control vector- (MCF7/Vec) or scramble shRNA-transfected cells (M3K/Scr). If FASN indeed mediates the anti-cancer effect of lansoprazole, over-expressing FASN should increase the IC_{50} value of lansoprazole. On the contrary, knocking down FASN should decrease the IC_{50} value of lansoprazole since there will be less FASN target to inhibit. Indeed, survival assay determined by colony formation showed that elevated FASN level enhanced breast cancer cell survival to lansoprazole, as indicated by the significant increase of IC_{50} from 4.8 μM in empty vector-transfected cells (MCF7/Vec) to 31.34 μM in FASN-over expressing cells (MCF7/FASN) (Figure 7A, 7C left panel). In addition, survival in M3k/Scr and M3k/shFASN cells were determined using methylene blue assay, since this pair of cells do not form colonies. As shown in Figure 7 below, while FASN expression was decreased, IC_{50} of lansoprazole significant dropped from 85.9 μM in control scramble shRNA-transfected cells (M3k/Scr) to 43 μM in stable FASN knockdown cells (M3k/shFASN) (Figure 7B, 7D left panel). These findings suggest that FASN indeed mediates the anti-cancer effect of lansoprazole. In addition, I tested whether FASN is a mediator of the anti-cancer effect of olaparib, a PARP-1 inhibitor, since FASN could regulate PARP-1 level (Figure 7A, 7B) [46]. Similarly, over-expressing FASN led to increased resistance to olaparib (Figure 7C, right panel) whereas knocking down FASN sensitized breast cancer cells to olaparib (Figure 7D, right panel). Taken together, these

results suggest that FASN is indeed a mediator of the anti-cancer effect of lansoprazole and the PARP-1 inhibitor, olaparib.

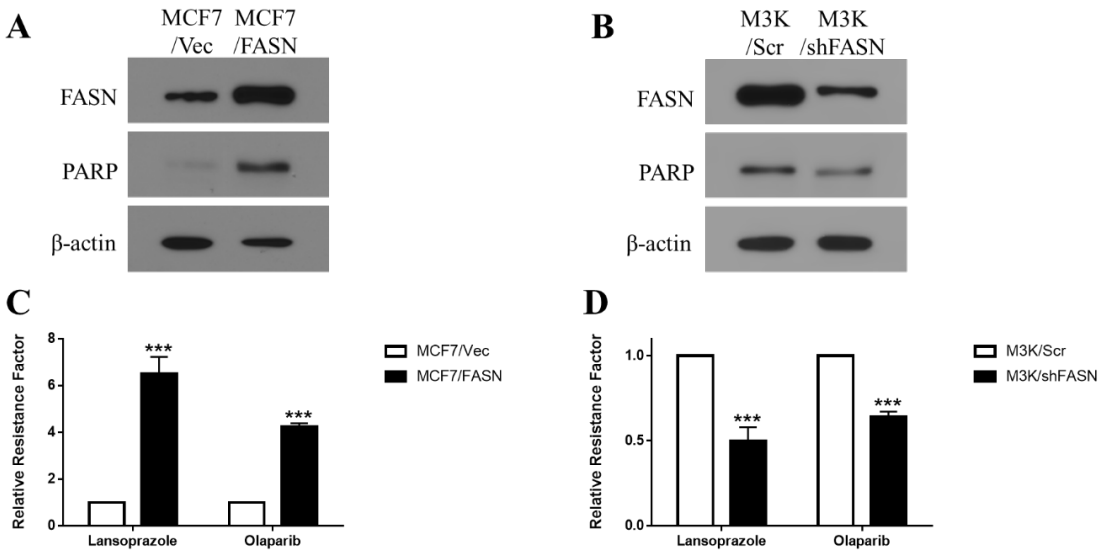

Figure 7: Effect of FASN level on sensitivity to lansoprazole and olaparib. Western blot analysis of FASN, PARP-1, and β-actin in (A) FASN-overexpressing cells (MCF7/FASN) and control vector-transfected cells (MCF7/Vec); (B) stable MCF7/AdVp3000 cells with FASN knockdown (M3k/shFASN) or scrambled control shRNA-transfection (M3k/Scr). Relative resistance factor of cell lines responds to lansoprazole and olaparib from (C) colony formation assay or (D) methylene blue assay. Relative resistance factor = IC_{50} of FASN up/down-regulating cells/IC_{50} of vector/scrambled shRNA-transfected control cells. Each bar is shown as the average of three independent experiments ± SD. *** $P < 0.001$.

H. FASN overexpression alleviates lansoprazole inhibition

We have shown that, in MCF7 and MDA-MB-468 cells, inhibiting FASN by lansoprazole reduced PARP level and NHEJ activity, eventually led to DNA damage. In this scenario, overexpression of ectopic FASN should be able to alleviate this pathway. As discussed above, over expressing and knocking down FASN decreased and increased the cellular sensitivity to lansoprazole treatment, respectively. To demonstrate that this change was through FASN inhibition, I tested PARP-1 level, NHEJ activity, and γ-H2AX level in vector transfected MCF7 and FASN over-expressing MCF7 cells following treatment with 10 μM lansoprazole or DMSO for 3 days. As shown in Figure 8, FASN overexpression maintained the similar level of PARP-1 and NHEJ activity with vector cell control group after treatment, whereas PAPR-1 level and NHEJ activity of vector treated group dropped significantly. γ-H2AX level was also found to be lower in FASN over-expressing MCF7 cells than vector transfected MCF7 cells. These findings provide additional evidence that FASN is a target of lansoprazole.

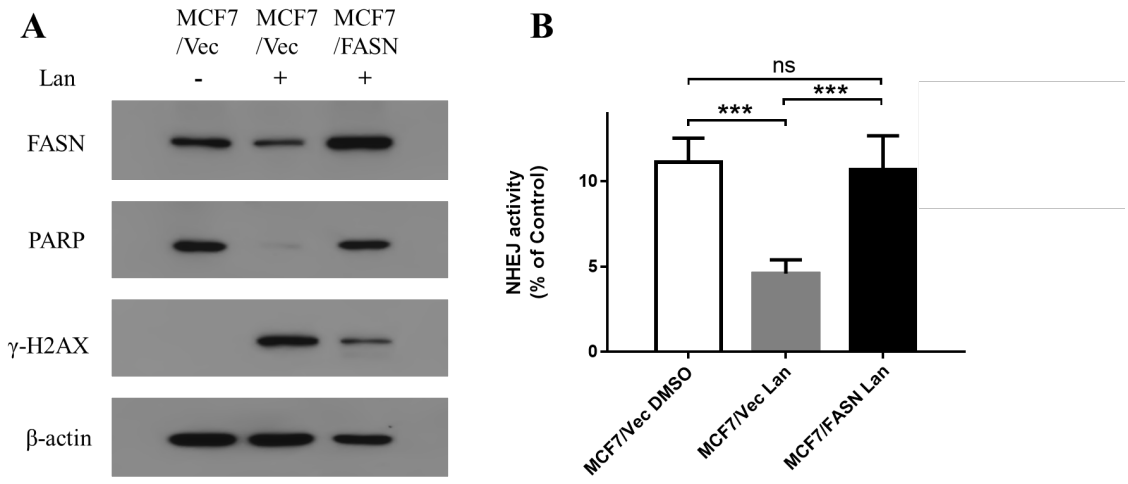

Figure 8: Effect of FASN overexpression on cellular response to lansoprazole. FASN-overexpressing cells (MCF7/FASN) and control vector-transfected cells (MCF7/Vec) were treated with DMSO or 10 μM lansoprazole for 3 days. Cells were collected for (A) western blot analysis of FASN, PARP-1, γ-H2AX, and β-actin, and (B) NHEJ activity using a host cell reactivation-based NHEJ assay. Each bar is shown as the average of three independent experiments ± SD. *** $P < 0.001$.

I. Lansoprazole induces apoptosis and disrupts cell cycle

Next, apoptosis and cell cycle distribution were analyzed using flow cytometry after treating MCF7 and MDA-MB-468 cells with 2.5 μM, 5 μM, 10 μM lansoprazole or DMSO for 3 days. As shown in Figure 9, overall apoptosis was observed in a dose-dependent way in both cell lines. Moreover, MCF7 cells showed G1 phase arrest (Figure 9C) while MDA-MB-468 cells showed S phase arrest (Figure 9D) also in a dose dependent manner. Both G1 arrest [62-66] and S phase arrest [59, 67-70] has been reported previously to associate with DNA damage. These findings indicate that by inhibiting FASN, lansoprazole induces cell cycle arrest and apoptosis in breast cancer cells.

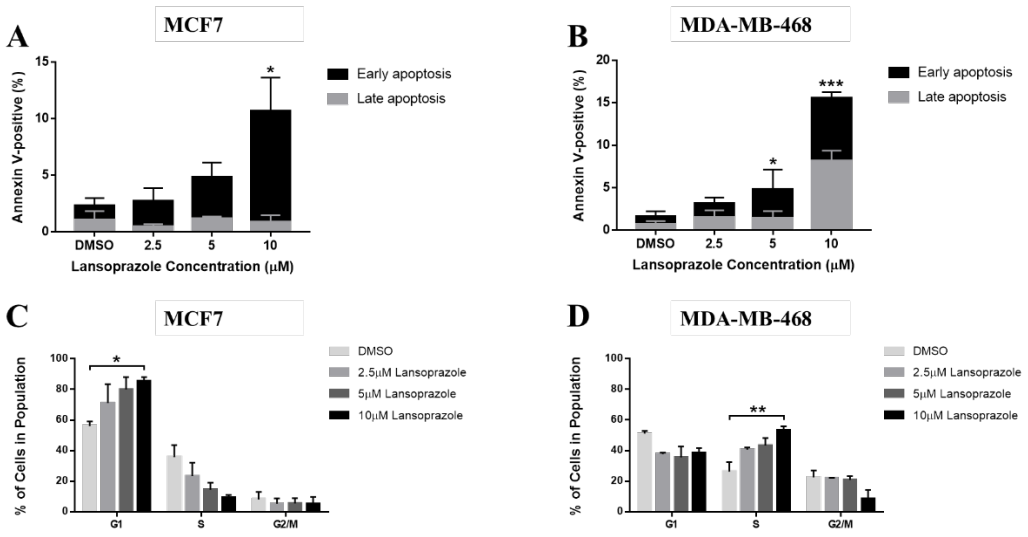

Figure 9: Apoptosis and cell cycle analysis by flow cytometry after lansoprazole treatment. Cells were treated with different concentrations of lansoprazole or DMSO for 3 days and stained with annexin V or propidium iodide. Percentages of early and late apoptosis are shown for MCF7 (A) and MDA-MB-468 (B). The percentages of cells from G1, S, and G2/M phases are shown for (C) MCF7 and (D) MDA-MB-468. Each bar is shown as the average of three independent experiments ± SD. * $P < 0.05$; ** $P < 0.01$; *** $P < 0.001$.

J. Doxorubicin and lansoprazole combination promotes γ-H2AX accumulation

To estimate if lansoprazole can sensitize doxorubicin in combination treatment, γ-H2AX level was detected as marker of DNA double strand break in western blot analysis. After treating MCF7 and MDA-MB-468 cells with lansoprazole (10 μM) and doxorubicin (50 nM or 200 nM), either alone or in combination for 3 days, cells exposed to both lansoprazole and doxorubicin had a dramatically increased γ-H2AX level compared to the cells given doxorubicin alone, as showed in Figure 10.

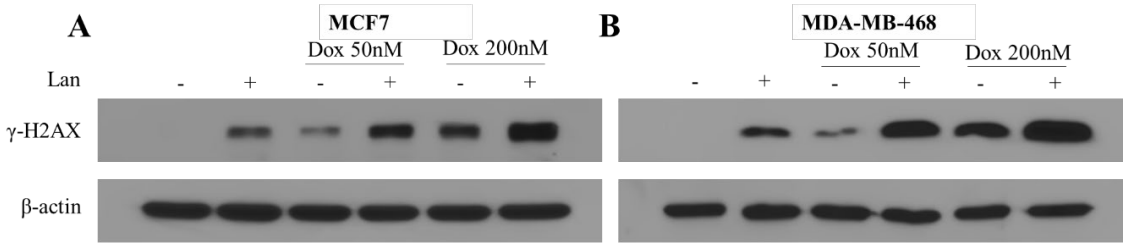

Figure 10: Lansoprazole promotes γ-H2AX accumulation when combined with doxorubicin. Western blot analyses of γ-H2AX in MCF7 (A) and MDA-MB-468 (B) cells treated with lansoprazole and doxorubicin alone or in combination.

K. Doxorubicin and lansoprazole combination achieves synergistic effect

To further estimate the synergistic effect of lansoprazole and doxorubicin, breast cancer cells were treated with lansoprazole and doxorubicin in combination using colony formation assay. The IC_{50} of doxorubicin in breast cancer cells was first determined (Figure 11A). MCF7 and MDA-MB-468 were selected for the combination study due to their relatively higher FASN level and better sensitivity to lansoprazole. Combination study was carried out in 3 different potency ratios of doxorubicin and lansoprazole: 1:3, 1:1, and 3:1. Combination treatments yielded significantly greater growth inhibition than either drug alone (Figure 11B, 11C). The isobologram analysis and combination-index analysis developed by Greco and Chou were used to confirm and quantify the synergism between lansoprazole and doxorubicin. Isobologram analysis provides a graphical presentation of the nature of interaction of two drugs, and combination-index analysis provides a quantitative measurement of the extent of drug interaction at a given effect level. Isobolograms were constructed for three defined effects of each drug: IC_{30}, IC_{50}, and IC_{70}, representing 30%, 50%, and 70% growth inhibition, respectively (Figure 11D). The line of additivity is constructed by connecting these two points with 30%, 50% and 70% growth inhibition of lansoprazole and doxorubicin. Concentrations of the two drugs used in combination to provide the same effect are showed in the same plot. Synergy, additivity, or antagonism is indicated when this point is located below, on, or above the line, respectively. For 1:3, 1:1, and 3:1 potency ratio, at 30%, 50%, and 70% growth inhibition in MCF7 and MDA-MB-468 cells, all combination points are located below the line of additivity. Combination-index values were calculated and plotted to correlated fractional effect from 0.3 to 0.7 to quantify synergy of drug combinations defined as additive effect (CI = 1),

synergism (CI < 1), and antagonism (CI > 1) (Figure 11E). CI values were summarized in Table 3. Both methods suggested strong synergy between doxorubicin and lansoprazole over a wide range of effects and combination ratio.

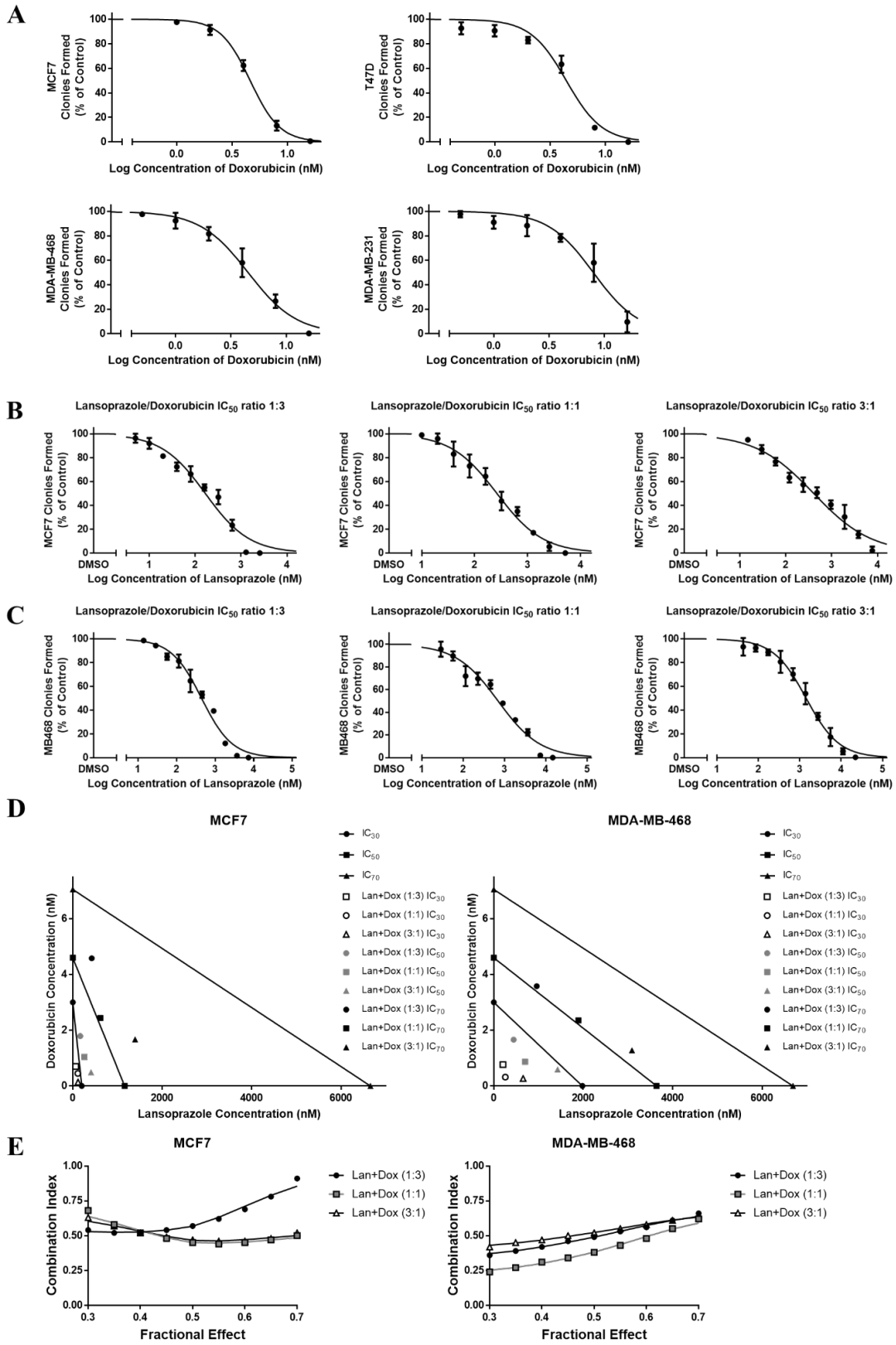
A
MCF7 Clonies Formed (% of Control)
T47D Clonies Formed (% of Control)
MDA-MB-468 Clonies Formed (% of Control)
MDA-MB-231 Clonies Formed (% of Control)
Log Concentration of Doxorubicin (nM)
B
Lansoprazole/Doxorubicin IC50 ratio 1:3
Lansoprazole/Doxorubicin IC50 ratio 1:1
Lansoprazole/Doxorubicin IC50 ratio 3:1
MCF7 Clonies Formed (% of Control)
Log Concentration of Lansoprazole (nM)
C
MB468 Clonies Formed (% of Control)
D
MCF7
MDA-MB-468
Doxorubicin Concentration (nM)
Lansoprazole Concentration (nM)
IC30
IC50
IC70
Lan+Dox (1:3) IC30
Lan+Dox (1:1) IC30
Lan+Dox (3:1) IC30
Lan+Dox (1:3) IC50
Lan+Dox (1:1) IC50
Lan+Dox (3:1) IC50
Lan+Dox (1:3) IC70
Lan+Dox (1:1) IC70
Lan+Dox (3:1) IC70
E
Combination Index
Fractional Effect
Lan+Dox (1:3)
Lan+Dox (1:1)
Lan+Dox (3:1)

Figure 11: Combination study of lansoprazole and doxorubicin. The ability of doxorubicin to inhibit cellular proliferation was measured by colony formation assay in (A) MCF7, T47D, MDA-MB468, and MDA-MB-231 cells. The ability of lansoprazole and doxorubicin combination to inhibit cellular proliferation at different potency ratios was tested in (B) MCF7 and (C) MDA-MB468 cells. Each point is shown as the average of three independent experiments ± SD. Isobologram analysis (D) and combination indexes at different fraction effect (E) are shown.

TABLE 3: Combination index at different fraction effect.

	Potency Ratio	Combination Index								
	Lan/Dox	IC_{30}	IC_{35}	IC_{40}	IC_{45}	IC_{50}	IC_{55}	IC_{60}	IC_{65}	IC_{70}
MCF7	1:3	0.54	0.52	0.52	0.54	0.57	0.62	0.69	0.78	0.91
	1:1	0.68	0.58	0.52	0.48	0.45	0.44	0.45	0.47	0.50
	3:1	0.63	0.57	0.52	0.49	0.47	0.46	0.46	0.48	0.52
MDA-MB-468	1:3	0.36	0.39	0.42	0.46	0.49	0.53	0.56	0.61	0.66
	1:1	0.24	0.27	0.31	0.34	0.38	0.43	0.48	0.55	0.62
	3:1	0.42	0.45	0.47	0.50	0.52	0.55	0.58	0.61	0.65

L. Lansoprazole sensitizes breast cancer cells to ionizing radiation

Radiation therapy is an important component in the local control of many tumor types including breast cancer. DNA double-strand breaks are responsible for the majority of ionizing radiation-induced cell killing in tumor tissue. But, the ability of breast cancer cells to upregulate DNA repair pathways promotes radiation resistance and tumor cell survival. Consequently, lansoprazole, which can reduce NHEJ activity by inhibiting FASN inhibition, was tested for its ability to sensitize IR treatment by examining γ-H2AX level and IC_{50} of IR using colony formation assay.

To detect γ-H2AX level, MCF7 and MDA-MB-468 cells were pre-treated with 10 μM lansoprazole or DMSO for 3 days and then treated without or with 5 Gy irradiation. Cells were then collected at 1 hour or 4 hours after IR. As shown in Figure 12A, cells had similar γ-H2AX level with or without lansoprazole pre-treatment 1 hour after IR. But 4 hours after IR, lansoprazole pre-treated cells had much higher γ-H2AX level comparing to cells only treated with IR.

For survival assay, cells pre-treated with or without lansoprazole for 3 days were seeded in 6 well plates, followed by exposure to different doses of IR and continuous culture for 14 days before staining and quantification of colonies formed. As shown in Figure 12B and Table 4, the IC_{50} values of IR in lansoprazole pre-treated group were significantly lower in both MCF7 and MDA-MB-468 cells, comparing to control-pretreated group. Thus, lansoprazole may sensitize cellular response to IR.

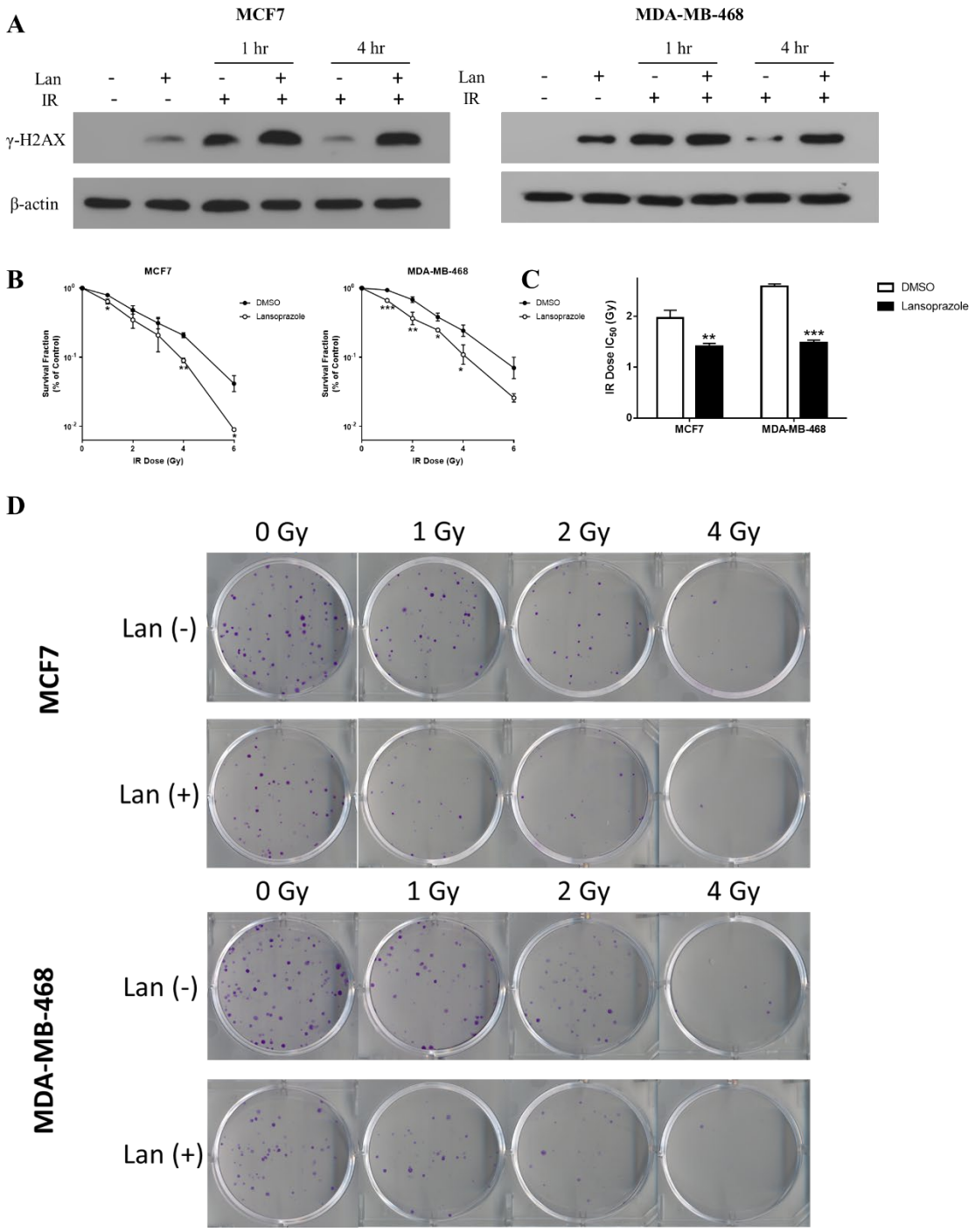

Figure 12: Lansoprazole hampers breast cancer cell γ-H2AX clearance and sensitizes IR treatment. (A) Western blot analyses of γ-H2AX in MCF7 and MDA-MB-468 cells treated with lansoprazole, IR, or in combination. (B) Dose-response curves of IR alone or combined with lansoprazole from colony formation assay. (C) The IC_{50} value of cellular

proliferation by IR alone or combined with lansoprazole is shown. Each point or bar is shown as the average of three independent experiments ± SD. * $P < 0.05$; ** $P < 0.01$; *** $P < 0.001$. (D) Representative scanned image showing different levels of colony formation in MCF7 and MDA-MB-468 cells treated with lansoprazole, IR, or in combination.

TABLE 4: IC_{50} of IR in combination with or without lansoprazole.

	DMSO	Lansoprazole	
	IC_{50} (Gy)	**IC_{50} (Gy)**	**P Value**
MCF7	1.96 ± 0.15	1.41 ± 0.06	0.004410959
MDA-MB-468	2.59 ± 0.05	1.48 ± 0.05	1.01707E-05

Conclusions and Discussion

Deregulated lipid biosynthesis is a characteristic feature of cancer and plays important roles in tumor cell development, growth, progression, and survival. Higher enzyme levels and activities in the lipid synthesis pathway are found in cancer cells. FASN, the key enzyme in *de novo* lipid biosynthesis, is a promising therapeutic target for cancer. In this study, PPIs as FASN inhibitors were evaluated. I found that PPIs can inhibit FASN activity and breast cancer cell proliferation dose-dependently. My data suggest that through inhibition of FASN, PPIs reduced PARP-1 level and NHEJ activity, resulting in increased DNA damage accumulation and sensitization of breast cancer cells to doxorubicin and IR treatments.

In FASN activity assay, all four PPIs inhibited FASN activity dose-dependently at the micromolar level. I found that lansoprazole and rabeprazole had lower IC_{50}s compared to omeprazole and pantoprazole. On the chemical structure side, omeprazole and pantoprazole have an extra methoxy/difluoromethoxy group on the 6th carbon of the benzimidazole, whereas lansoprazole and rabeprazole lack this extra moiety. This may indicate that the extra group on the 6th carbon can reduce the binding affinity of PPIs to FASN. In survival assays, lansoprazole was shown to have the highest potency in all four cell lines tested. On the other hand, rabeprazole, which had similar IC_{50} with lansoprazole in FASN activity assay, had much higher IC_{50} in survival assay. This could be due to the fact that rabeprazole is the most hydrophilic and water-soluble among the PPIs tested, making it harder to cross the cellular membrane than lansoprazole and to reach the cytosolic FASN protein. In addition, rabeprazole's low membrane penetration could likely explain why its IC_{50} had a poorer correlation coefficient to relative cellular FASN level comparing

to lansoprazole. Thus, lansoprazole, for its consistently better performance in FASN activity assay, survival assay, and correlation study, was selected as the best PPI and evaluated in further experiments.

I next tested the impact of ectopically varying FASN levels on breast cancer cells' sensitivity to lansoprazole. I observed higher lansoprazole IC_{50} in stable FASN over-expressing MCF7 cells than control vector cells and lower lansoprazole IC_{50} in stable FASN partial knock-down M3k cells than control scramble shRNA-transfected cells. This seemed to be opposite to the findings from the correlation study, in which cell line with higher FASN level was more sensitive to lansoprazole. One possible explanation could be the endogenous FASN levels in parental breast cancer cell lines were the result of adaptation of cancer cells during mutation, development, and growth, representing roughly how much FASN that specific cell line requires. Thus, cell lines with higher endogenous FASN levels could be more dependent on *de novo* fatty-acid synthesis than cell lines with lower FASN level and as such, exhibit higher sensitivity to FASN inhibition. However, when FASN is ectopically over-expressed by transfection, it could give cancer cells a better chance to survive the treatment of FASN inhibitor, due to the extra FASN available. Another possibility may be that lansoprazole may have other targets in the cells and the overexpressed FASN may protect those targets from the effect of lansoprazole.

Previously, our lab has demonstrated that FASN mediated breast cancer cells' resistance and survival to genotoxic treatments is through up-regulated PARP-1and NHEJ activity. In this work, I tested the ability of lansoprazole to reverse this resistance by inhibiting FASN activity, and therefore to sensitize breast cancer cells to DNA damaging insults (Figure 13). After treating breast cancer cells with lansoprazole, I observed significant PARP-1 level

reduction at both mRNA and protein levels. Lansoprazole treatment also significantly reduced NHEJ repair activity and increased γ-H2AX level, indicating elevated DSB accumulation. When combined with either doxorubicin or ionizing radiation, cells treated with lansoprazole had higher γ-H2AX level and lower IC_{50} to doxorubicin and IR than treated with doxorubicin or IR alone. These novel findings may suggest the possibility that utilizing lansoprazole, an FDA-approved OTC drug in combination therapy, has the potential to benefit breast cancer patients not only by reducing the dose of toxic DNA damaging agents or IR, but also by regaining sensitivity in resistant breast cancers.

A few other groups have also reported that PPIs inhibit cancer cell growth using *in vitro* and animal models. Most studies concluded that PPIs exert their anti-cancer activity through proton pump inhibition via the disulfide bond, not by targeting the gastric H^+, K^+-ATPase, but via the neoplastic vacuolar H^+-ATPase (V-ATPase), a type of proton pump expressed by cancer cells [71-74]. Cancer cells have unique metabolism and dysregulated pH compared to normal cells, known as the Warburg effect, thus up-regulated proton extrusion activity via V-ATPase is crucial for tumor cells to survive this unfavorable condition. It is believed that inhibiting V-ATPase with PPIs reduces proton extrusion and induces sensitization of cancer cells to chemotherapeutics. In addition, Azzarito et al. suggest that the low pH of tumor microenvironment is also suitable for activation of PPIs [53]. This mechanism seems valid to explain the anti-cancer activity of PPIs.

However, questions remain about this V-ATPase theory, particularly regarding the activation step of PPIs required for their V-ATPase inhibition activity. As we know, PPIs are prodrugs with alkaline properties, and must undergo two steps of protonation to become fully activated thiophilic sulphenamides. The pKa1 of PPIs are around 4 and pKa2 are

below 1. The only space in the body with a pH below 4.0 to allow selective accumulation and activation of PPIs is inside the gastric parietal cells, the traditional target of PPIs. In addition, once activated, PPIs become less membrane permeable, which makes it more difficult to transport out of parietal cells after activation. Activation of PPIs at the tumor microenvironment would be too slow to allow the build-up of any effective concentration of sulfonamide, plus PPIs activated at gastric parietal cell could not be transported to tumor sites, thus the majority of PPIs at the tumor site are un-activated and incapable of inhibiting V-ATPase, even when given orally [75-79]. These evidences beg to argue that alternative mechanisms to explain PPIs' anti-cancer activity exist. On the other hand, the commercial cell culture media used in our studies was buffered between 7.0 to 7.4. Under these neutral environments, I have observed that even inactivated PPIs still exhibited anti-cancer ability. Previous study in our lab showed that PPI treatment did not affect the intracellular or extracellular pH [46]. In addition, most data reported from other groups were also generated using neutrally-buffered media. Even for the study which claims the low pH of tumor microenvironment is suitable for a full PPI activation, the lowest extracellular and cytosolic pH they could achieve using non-buffered media was around 6.5, which is still much higher than necessary for PPI activation [53]. In reports using animal models where PPIs were given to mice via intraperitoneal or intravenous injection which would not allow activation at the stomach, anti-tumor activity was also observed. Our study here presents a novel mechanism by which PPIs could sensitize breast cancer cells without protonating activation, namely via targeting FASN.

There are several experiments that could be performed as a follow-up to this work. Firstly, we could perform combination study of lansoprazole with either doxorubicin or IR in

mouse xenograft tumor models. We will determine if lansoprazole also reduces the protein and mRNA level of PARP-1 in xenograft tumors as it did *in vitro*. Secondly, we will test the optical isomers, derivatives, and metabolites of PPIs to search for compounds with higher potency towards FASN inhibition. Thirdly, we will determine if there is any synergistic effect between lansoprazole and PARP inhibitors to sensitize breast cancer cells to DNA damaging treatment, based on our data suggesting they could function in the same pathway (Figure 13). Finally, we will attempt to co-crystalize PPIs with FASN TE domain to map out the specific interaction between FASN and PPIs, which would provide basis for the modification of current PPIs to become more specific and effective FASN inhibitors.

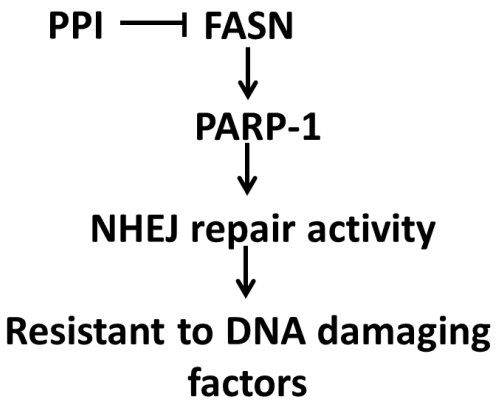

Figure 13: Schematic representation of the proposed mechanism by which PPIs, via FASN inhibition, sensitize breast cancer cells to DNA damaging treatments.

References

1. Wakil, S.J., *Fatty acid synthase, a proficient multifunctional enzyme.* Biochemistry, 1989. **28**(11): p. 4523-30.
2. Smith, S., *The animal fatty acid synthase: one gene, one polypeptide, seven enzymes.* FASEB J, 1994. **8**(15): p. 1248-59.
3. Maier, T., S. Jenni, and N. Ban, *Architecture of mammalian fatty acid synthase at 4.5 A resolution.* Science, 2006. **311**(5765): p. 1258-62.
4. Maier, T., M. Leibundgut, and N. Ban, *The crystal structure of a mammalian fatty acid synthase.* Science, 2008. **321**(5894): p. 1315-22.
5. Hellerstein, M.K., J.M. Schwarz, and R.A. Neese, *Regulation of hepatic de novo lipogenesis in humans.* Annu Rev Nutr, 1996. **16**: p. 523-57.
6. Hellerstein, M.K., *De novo lipogenesis in humans: metabolic and regulatory aspects.* Eur J Clin Nutr, 1999. **53 Suppl 1**: p. S53-65.
7. Hillgartner, F.B., L.M. Salati, and A.G. Goodridge, *Physiological and molecular mechanisms involved in nutritional regulation of fatty acid synthesis.* Physiol Rev, 1995. **75**(1): p. 47-76.
8. Kersten, S., *Mechanisms of nutritional and hormonal regulation of lipogenesis.* EMBO Rep, 2001. **2**(4): p. 282-6.
9. Kuhajda, F.P., *Fatty-acid synthase and human cancer: new perspectives on its role in tumor biology.* Nutrition, 2000. **16**(3): p. 202-8.
10. Kusakabe, T., et al., *Fatty acid synthase is expressed mainly in adult hormone-sensitive cells or cells with high lipid metabolism and in proliferating fetal cells.* J Histochem Cytochem, 2000. **48**(5): p. 613-22.
11. Bobrow, L.G., et al., *The classification of ductal carcinoma in situ and its association with biological markers.* Semin Diagn Pathol, 1994. **11**(3): p. 199-207.
12. Jensen, V., et al., *The prognostic value of oncogenic antigen 519 (OA-519) expression and proliferative activity detected by antibody MIB-1 in node-negative breast cancer.* J Pathol, 1995. **176**(4): p. 343-52.
13. Visca, P., et al., *Fatty acid synthase (FAS) is a marker of increased risk of recurrence in lung carcinoma.* Anticancer Res, 2004. **24**(6): p. 4169-73.
14. Geisler, J., et al., *Changes in bone and lipid metabolism in postmenopausal women with early breast cancer after terminating 2-year treatment with exemestane: a randomised, placebo-controlled study.* Eur J Cancer, 2006. **42**(17): p. 2968-75.
15. Hilvo, M., et al., *Novel theranostic opportunities offered by characterization of altered membrane lipid metabolism in breast cancer progression.* Cancer Res, 2011. **71**(9): p. 3236-45.
16. Jung, Y.Y., H.M. Kim, and J.S. Koo, *Expression of Lipid Metabolism-Related Proteins in Metastatic Breast Cancer.* PLoS One, 2015. **10**(9): p. e0137204.
17. Kim, S., Y. Lee, and J.S. Koo, *Differential expression of lipid metabolism-related proteins in different breast cancer subtypes.* PLoS One, 2015. **10**(3): p. e0119473.
18. Sidorenko, L.N., et al., *[Lipid and protein metabolism in breast cancer].* Vopr Onkol, 1982. **28**(4): p. 79-81.
19. Wang, J., et al., *Lipid metabolism genes in contralateral unaffected breast and estrogen receptor status of breast cancer.* Cancer Prev Res (Phila), 2013. **6**(4): p. 321-30.

20. Santos, C.R. and A. Schulze, *Lipid metabolism in cancer.* FEBS J, 2012. **279**(15): p. 2610-23.
21. Currie, E., et al., *Cellular fatty acid metabolism and cancer.* Cell Metab, 2013. **18**(2): p. 153-61.
22. Yang, Y., et al., *Role of fatty acid synthase in gemcitabine and radiation resistance of pancreatic cancers.* Int J Biochem Mol Biol, 2011. **2**(1): p. 89-98.
23. Liu, H., et al., *Fatty acid synthase causes drug resistance by inhibiting TNF-alpha and ceramide production.* J Lipid Res, 2013. **54**(3): p. 776-85.
24. Wu, X., et al., *FASN regulates cellular response to genotoxic treatments by increasing PARP-1 expression and DNA repair activity via NF-kappaB and SP1.* Proc Natl Acad Sci U S A, 2016.
25. Kim, M.Y., T. Zhang, and W.L. Kraus, *Poly(ADP-ribosyl)ation by PARP-1: 'PAR-laying' NAD+ into a nuclear signal.* Genes Dev, 2005. **19**(17): p. 1951-67.
26. Redon, C.E., et al., *Histone gammaH2AX and poly(ADP-ribose) as clinical pharmacodynamic biomarkers.* Clin Cancer Res, 2010. **16**(18): p. 4532-42.
27. Luo, X. and W.L. Kraus, *On PAR with PARP: cellular stress signaling through poly(ADP-ribose) and PARP-1.* Genes Dev, 2012. **26**(5): p. 417-32.
28. Kakarougkas, A. and P.A. Jeggo, *DNA DSB repair pathway choice: an orchestrated handover mechanism.* Br J Radiol, 2014. **87**(1035): p. 20130685.
29. Gupta, R., et al., *DNA Repair Network Analysis Reveals Shieldin as a Key Regulator of NHEJ and PARP Inhibitor Sensitivity.* Cell, 2018. **173**(4): p. 972-988 e23.
30. Kuhajda, F.P., et al., *Fatty acid synthesis: a potential selective target for antineoplastic therapy.* Proc Natl Acad Sci U S A, 1994. **91**(14): p. 6379-83.
31. Liu, X., et al., *Inhibition of the phosphatidylinositol 3-kinase/Akt pathway sensitizes MDA-MB468 human breast cancer cells to cerulenin-induced apoptosis.* Mol Cancer Ther, 2006. **5**(3): p. 494-501.
32. Pizer, E.S., et al., *Inhibition of fatty acid synthesis induces programmed cell death in human breast cancer cells.* Cancer Res, 1996. **56**(12): p. 2745-7.
33. Pizer, E.S., et al., *Malonyl-coenzyme-A is a potential mediator of cytotoxicity induced by fatty-acid synthase inhibition in human breast cancer cells and xenografts.* Cancer Res, 2000. **60**(2): p. 213-8.
34. Menendez, J.A., et al., *Pharmacological inhibition of fatty acid synthase (FAS): a novel therapeutic approach for breast cancer chemoprevention through its ability to suppress Her-2/neu (erbB-2) oncogene-induced malignant transformation.* Mol Carcinog, 2004. **41**(3): p. 164-78.
35. Vazquez-Martin, A., et al., *Pharmacological blockade of fatty acid synthase (FASN) reverses acquired autoresistance to trastuzumab (Herceptin by transcriptionally inhibiting 'HER2 super-expression' occurring in high-dose trastuzumab-conditioned SKBR3/Tzb100 breast cancer cells.* Int J Oncol, 2007. **31**(4): p. 769-76.
36. Puig, T., et al., *Fatty acid metabolism in breast cancer cells: differential inhibitory effects of epigallocatechin gallate (EGCG) and C75.* Breast Cancer Res Treat, 2008. **109**(3): p. 471-9.
37. Nie, F., et al., *Apoptotic effect of tannic acid on fatty acid synthase over-expressed human breast cancer cells.* Tumour Biol, 2016. **37**(2): p. 2137-43.

38. Menendez, J.A. and R. Lupu, *Fatty acid synthase regulates estrogen receptor-alpha signaling in breast cancer cells.* Oncogenesis, 2017. **6**(2): p. e299.
39. Kridel, S.J., et al., *Orlistat is a novel inhibitor of fatty acid synthase with antitumor activity.* Cancer Res, 2004. **64**(6): p. 2070-5.
40. Pemble, C.W.t., et al., *Crystal structure of the thioesterase domain of human fatty acid synthase inhibited by Orlistat.* Nat Struct Mol Biol, 2007. **14**(8): p. 704-9.
41. Carvalho, M.A., et al., *Fatty acid synthase inhibition with Orlistat promotes apoptosis and reduces cell growth and lymph node metastasis in a mouse melanoma model.* Int J Cancer, 2008. **123**(11): p. 2557-65.
42. Sadowski, M.C., et al., *The fatty acid synthase inhibitor triclosan: repurposing an anti-microbial agent for targeting prostate cancer.* Oncotarget, 2014. **5**(19): p. 9362-81.
43. Lee, H.R., et al., *Progression of breast cancer cells was enhanced by endocrine-disrupting chemicals, triclosan and octylphenol, via an estrogen receptor-dependent signaling pathway in cellular and mouse xenograft models.* Chem Res Toxicol, 2014. **27**(5): p. 834-42.
44. Sippel, K.H., et al., *Crystal structure of the human fatty acid synthase enoyl-acyl carrier protein-reductase domain complexed with triclosan reveals allosteric protein-protein interface inhibition.* J Biol Chem, 2014. **289**(48): p. 33287-95.
45. Jones, S.F. and J.R. Infante, *Molecular Pathways: Fatty Acid Synthase.* Clin Cancer Res, 2015. **21**(24): p. 5434-8.
46. Fako, V.E., et al., *Repositioning proton pump inhibitors as anticancer drugs by targeting the thioesterase domain of human fatty acid synthase.* J Med Chem, 2015. **58**(2): p. 778-84.
47. Shin, J.M. and N. Kim, *Pharmacokinetics and pharmacodynamics of the proton pump inhibitors.* J Neurogastroenterol Motil, 2013. **19**(1): p. 25-35.
48. Yu, M., et al., *Influence of the proton pump inhibitor lansoprazole on distribution and activity of doxorubicin in solid tumors.* Cancer Sci, 2015. **106**(10): p. 1438-47.
49. Wang, B.Y., et al., *Intermittent high dose proton pump inhibitor enhances the antitumor effects of chemotherapy in metastatic breast cancer.* J Exp Clin Cancer Res, 2015. **34**: p. 85.
50. Patel, K.J., et al., *Use of the proton pump inhibitor pantoprazole to modify the distribution and activity of doxorubicin: a potential strategy to improve the therapy of solid tumors.* Clin Cancer Res, 2013. **19**(24): p. 6766-76.
51. Spugnini, E.P., et al., *High dose lansoprazole combined with metronomic chemotherapy: a phase I/II study in companion animals with spontaneously occurring tumors.* J Transl Med, 2014. **12**: p. 225.
52. Zhang, S., Y. Wang, and S.J. Li, *Lansoprazole induces apoptosis of breast cancer cells through inhibition of intracellular proton extrusion.* Biochem Biophys Res Commun, 2014. **448**(4): p. 424-9.
53. Azzarito, T., et al., *Lansoprazole induces sensitivity to suboptimal doses of paclitaxel in human melanoma.* Cancer Lett, 2015. **356**(2 Pt B): p. 697-703.
54. Lelliott, C.J., et al., *Transcript and metabolite analysis of the effects of tamoxifen in rat liver reveals inhibition of fatty acid synthesis in the presence of hepatic steatosis.* FASEB J, 2005. **19**(9): p. 1108-19.

55. Greco, W.R., G. Bravo, and J.C. Parsons, *The search for synergy: a critical review from a response surface perspective.* Pharmacol Rev, 1995. **47**(2): p. 331-85.
56. Chou, T.C., *Theoretical basis, experimental design, and computerized simulation of synergism and antagonism in drug combination studies.* Pharmacol Rev, 2006. **58**(3): p. 621-81.
57. Chou, T.C., *Drug combination studies and their synergy quantification using the Chou-Talalay method.* Cancer Res, 2010. **70**(2): p. 440-6.
58. Zhao, L., J.L. Au, and M.G. Wientjes, *Comparison of methods for evaluating drug-drug interaction.* Front Biosci (Elite Ed), 2010. **2**: p. 241-9.
59. Zhang, W.H., et al., *DNA damage-induced S phase arrest in human breast cancer depends on Chk1, but G2 arrest can occur independently of Chk1, Chk2 or MAPKAPK2.* Cell Cycle, 2008. **7**(11): p. 1668-77.
60. Allen, C., et al., *More forks on the road to replication stress recovery.* J Mol Cell Biol, 2011. **3**(1): p. 4-12.
61. Zhan, N., et al., *Inhibition of FASN expression enhances radiosensitivity in human non-small cell lung cancer.* Oncol Lett, 2018. **15**(4): p. 4578-4584.
62. Di Leonardo, A., et al., *DNA damage triggers a prolonged p53-dependent G1 arrest and long-term induction of Cip1 in normal human fibroblasts.* Genes Dev, 1994. **8**(21): p. 2540-51.
63. Kastan, M.B. and S.J. Kuerbitz, *Control of G1 arrest after DNA damage.* Environ Health Perspect, 1993. **101 Suppl 5**: p. 55-8.
64. Orth, J.D., et al., *Prolonged mitotic arrest triggers partial activation of apoptosis, resulting in DNA damage and p53 induction.* Mol Biol Cell, 2012. **23**(4): p. 567-76.
65. Pellegata, N.S., et al., *DNA damage and p53-mediated cell cycle arrest: a reevaluation.* Proc Natl Acad Sci U S A, 1996. **93**(26): p. 15209-14.
66. Shapiro, G.I., et al., *p16INK4A participates in a G1 arrest checkpoint in response to DNA damage.* Mol Cell Biol, 1998. **18**(1): p. 378-87.
67. Yu, C.C., et al., *Norcantharidin triggers cell death and DNA damage through S-phase arrest and ROS-modulated apoptotic pathways in TSGH 8301 human urinary bladder carcinoma cells.* Int J Oncol, 2012. **41**(3): p. 1050-60.
68. Wei, J.H., et al., *Water-soluble oxoglaucine-Y(III), Dy(III) complexes: in vitro and in vivo anticancer activities by triggering DNA damage, leading to S phase arrest and apoptosis.* Dalton Trans, 2015. **44**(25): p. 11408-19.
69. Wang, K., et al., *Induction of S-Phase Arrest in Human Glioma Cells by Selenocysteine, a Natural Selenium-Containing Agent Via Triggering Reactive Oxygen Species-Mediated DNA Damage and Modulating MAPKs and AKT Pathways.* Neurochem Res, 2016. **41**(6): p. 1439-47.
70. Li, D., et al., *GADD45a Regulates Olaquindox-Induced DNA Damage and S-Phase Arrest in Human Hepatoma G2 Cells via JNK/p38 Pathways.* Molecules, 2017. **22**(1).
71. Tavares-Valente, D., et al., *Cancer cell bioenergetics and pH regulation influence breast cancer cell resistance to paclitaxel and doxorubicin.* J Bioenerg Biomembr, 2013. **45**(5): p. 467-75.
72. Luciani, F., et al., *Effect of proton pump inhibitor pretreatment on resistance of solid tumors to cytotoxic drugs.* J Natl Cancer Inst, 2004. **96**(22): p. 1702-13.

73. Lee, Y.Y., et al., *Proton pump inhibitors enhance the effects of cytotoxic agents in chemoresistant epithelial ovarian carcinoma.* Oncotarget, 2015. **6**(33): p. 35040-50.
74. Lugini, L., et al., *Proton pump inhibitors while belonging to the same family of generic drugs show different anti-tumor effect.* J Enzyme Inhib Med Chem, 2016. **31**(4): p. 538-45.
75. Olbe, L., *Proton pump inhibitors*. Milestones in drug therapy. 1999, Basel ; Boston: Birkhauser. x, 251 p.
76. Hellstrom, P.M. and S. Vitols, *The choice of proton pump inhibitor: does it matter?* Basic Clin Pharmacol Toxicol, 2004. **94**(3): p. 106-11.
77. Shin, J.M., Y.M. Cho, and G. Sachs, *Chemistry of covalent inhibition of the gastric (H+, K+)-ATPase by proton pump inhibitors.* J Am Chem Soc, 2004. **126**(25): p. 7800-11.
78. Sachs, G., J.M. Shin, and C.W. Howden, *Review article: the clinical pharmacology of proton pump inhibitors.* Aliment Pharmacol Ther, 2006. **23 Suppl 2**: p. 2-8.
79. Kromer, W., et al., *Differences in pH-dependent activation rates of substituted benzimidazoles and biological in vitro correlates.* Pharmacology, 1998. **56**(2): p. 57-70.

Curriculum Vitae

Chao Wang

EDUCATION

2015 - 2018	Master of Science in Pharmacology Indiana University. Cumulative GPA: 3.97/4.0
2006 - 2008	Master's student in Pharmaceutics Shenyang Pharmaceutical University
2001 - 2005	Bachelor of Engineering in Pharmaceutics Shenyang Pharmaceutical University

RESEARCH EXPERIENCE

Indiana University School of Medicine
Graduate Research Assistant: 2015-2018
Department of Pharmacology: Dr. J. T. Zhang

1. Utilization of proton pump inhibitors in breast cancer combination regimen by targeting fatty acid synthase.
2. Synergistic effect of proton pump inhibitors and PARP inhibitors combinational therapy in triple-negative breast cancer cells.
3. Role of fatty acid synthase (FASN) in DNA repair and breast cancer chemo-resistance.
4. Role of eIF3a in cellular response to IR treatment by regulating synthesis of proteins important for NHEJ repair of DSBs.

Indiana University School of Medicine
Graduate Research Assistant: 2015-2016
Department of Pharmacology: Dr. J.Y. Liu

1. Screening of small molecule inhibitors of oncoproteins and pro-proliferation proteins as target cancer therapeutics.
2. Novel benzimidazole analogs suppress cancer cell proliferation by inhibiting human fatty acid synthase

Shenyang Pharmaceutical University School of Pharmaceutical sciences
Graduate Research Assistant: 2006-2008
Department of Pharmaceutics: Dr. S.M. Li

1. Development of a novel drug-delivery formulation for the active anti-inflammatory ingredient of a Chinese medicinal plant, rhodiola rosea.

PUBLICATIONS

1. Wu X, Dong ZZ, Wang CJ, Barlow LJ, Fako V, Serrano MA, Zou Y,Liu JY, Zhang JT. FASN regulates cellular response to genotoxic treatments by increasing PARP-

1 expression and DNA repair activity via NF-kappa B and SP1. PNAS. 2016 113: E6965-E6973.

2. Huang W, Dong Z, Chen Y, Wang F, Wang CJ, Peng H, He Y, Hangoc G, Pollok K, Sandusky G, Fu XY, Broxmeyer HE, Zhang ZY, Liu JY, Zhang JT. Small-molecule inhibitors targeting the DNA-binding domain of STAT3 suppress tumor growth, metastasis and STAT3 target gene expression in vivo. Oncogene. 2016 Feb 11;35(6):802
3. Tumia RAH*, Wang CJ*, Dong ZZ, Dong TH, Zhang JT. eIF3a Sensitizes Cellular Response to Ionizing Radiation by Regulating Synthesis of NHEJ Repair Proteins. *Co-first author. (In Minor Revision to Oncotarget).
4. Wang CJ*, Li DR*, Liu JY, Zhang JT. Utilization of proton pump inhibitors in breast cancer neo-adjuvant regimen by targeting fatty acid synthase. *Co-first author. (Manuscript in preparation)
5. Wang CJ, Dong ZZ, Liu JY. Novel Benzimidazole analogs with Antitumor Activity targeting human fatty acid synthase. (Manuscript in preparation)